4×1 reconstruction of indium deposited on vicinal Si(111) surfaces

J. L. Stevens, M. S. Worthington, and I. S. T. Tsong
Department of Physics and Astronomy, Arizona State University, Tempe, Arizona 85287
(Received 7 July 1992; revised manuscript received 2 September 1992)

The Si(111)-(4×1) In reconstruction normally exists in three domains of double-row ridges along three equivalent $\langle \bar{1}10 \rangle$ directions on a flat Si(111) substrate. Using vicinal Si(111) surfaces as substrates, scanning-tunneling-microscopy images show the existence of only a single domain of the (4×1) reconstruction with the double rows aligning with the $[\bar{1}10]$ step edges when the surface is misoriented toward the $[\bar{1}\,\bar{1}2]$ direction. When the vicinal sample is misoriented toward the opposite, i.e., $[11\bar{2}]$, direction, however, all three domains are present. We performed impact-collision ion-scattering spectrometry experiments on the single-domain surface and the results confirm a model in which In adatoms occupy H_3 and T_4 sites with $\frac{1}{2}$-monolayer coverage.

I. INTRODUCTION

In 1964, Lander and Morrison[1,2] conducted the first adsorption studies by low-energy electron diffraction (LEED) of group-III metals on silicon surfaces and they reported eight reconstructions of indium (In) on Si(111) including $\sqrt{3}\times\sqrt{3}$ and 4×1. The $\sqrt{3}\times\sqrt{3}$ reconstructions induced on Si(111) are common among group-III metals, Al, Ga, and In, but the 4×1 geometry is unique to In. The first scanning-tunneling-microscopy (STM) studies by Nogami and co-workers[3,4] reveal that the 4×1 structure consists of ridges of double rows of atoms running along $\langle \bar{1}10 \rangle$ directions, yielding three equivalent orientations on the threefold symmetric Si(111) surface. Based on these STM studies, we set out to determine the atomic structure of the 4×1 geometry using the technique of impact-collision ion-scattering spectrometry (ICISS).[5] Based on our ICISS results, we proposed a model in which the In atoms occupy both H_3 and T_4 sites with $\frac{1}{2}$-monolayer (ML) coverage[5] consistent with the range of coverage, 0.5–1.2 ML, assigned by various workers[4,6–8] for the 4×1 reconstruction. However, due to complications arising from scattering from the three equivalent 4×1 domains, our mixed-site model was not completely unequivocal. To overcome the three-domain difficulty, Nakamura and co-workers[8] used a reflection high-energy electron-diffraction microprobe to analyze a smaller region on the surface containing a single 4×1 domain. From their results, Nakamura, Anno, and Kono[8] proposed a structural model with 1-ML In coverage, with the In atoms occupying H_3, T_4, and bridge sites.

While studying metal epitaxy with LEED, Bauer[9] noticed that near the edges of crystals where the surface was vicinal due to polishing and lapping, the reconstructions showed preferred orientations. This effect of step-edge pinned reconstruction was also observed by Akinci, Ohno, and Williams[10] in the $(\sqrt{19}\times\sqrt{19})$Ni reconstructions on misoriented surfaces of Si(111). In an attempt to produce a single (4×1)In domain for study by ICISS, we used Si(111) substrates which were intentionally misoriented 2.6° off axis towards $[\bar{1}\,\bar{1}2]$ (i.e., the outward normal to the step riser is $[\bar{1}\,\bar{1}2]$) and $[11\bar{2}]$ directions, yielding a vicinal surface for deposition of In. The single 4×1 domain will provide greatly simplified scattering conditions for ICISS, which will help to resolve the discrepancy between the different models proposed by us[5] and Nakamura, Anno, and Kono.[8]

II. EXPERIMENT

The vicinal surfaces of Si(111) were cut from an *n*-type wafer of 0.02-Ω cm resistivity with the surface normal misoriented by 2.6° towards either the $[\bar{1}\,\bar{1}2]$ or $[11\bar{2}]$ direction. Henceforth we refer to the $[\bar{1}\,\bar{1}2]$ misorientation as the type-*A* surface and the $[11\bar{2}]$ as type *B*.

The Si sample was rinsed in methanol, then flashed to approximately 1200 °C for a few seconds to remove the oxide layer while maintaining the pressure in the vacuum chamber at $\leq 1\times10^{-9}$ Torr. This procedure was repeated several times. For the type-*A* surface, the sample was quickly cooled to 920 °C, then slowly cooled at 1°/sec to 830 °C before quenching to room temperature. This procedure produced 7×7 terraces with widths from 90 to 150 Å separated primarily by single-atom height steps. Approximately 20% triple-atom height steps were also present. For the type-*B* surface, this same procedure produced terraces ~500 Å wide separated by regions of bunched, narrow (≤10-Å) terraces containing 10–15 steps per bunch. The occurrence of single and triple steps on the type-*A* and step bunching on type-*B* vicinal surfaces is in agreement with observations of Williams and Bartelt.[11] When a type-*B* surface was quenched rapidly from 1200 °C to room temperature, some regions of ~100-Å-wide terraces separated by single-atom height steps were produced.

Indium was deposited at a rate of ~1 Å/min (1 Å=0.49 ML) and monitored by a quartz-crystal monitor. A variety of coverages from 0.7 to 2.0 ML were deposited and then annealed at 350 °C–450 °C for 10–15 min. No 4×1 reconstruction was observed below 0.7-ML deposition. The best result for the production of the 4×1

reconstruction was deposition of 1 ML of In followed by annealing at 400 °C for 10 min. After annealing to obtain the 4×1 surface, the step height distribution, i.e., single or triple, remained the same. Step bunching or faceting was not observed. However, some, but not all, step edges changed from straight to meandering, possibly due to the combined effect of In adsorption and annealing.

STM images of the 4×1 reconstruction were taken on both the type-*A* and type-*B* surfaces. ICISS experiments, however, were carried out on the type-*A* surface only. The STM and ICISS experiments were conducted in separate ultrahigh-vacuum chambers. Each of these chambers contained its own *in situ* annealing and deposition facilities. The ICISS chamber was also equipped with a reverse-view LEED which was used to confirm the existence of surface order prior to ion scattering. The procedure for carrying out ICISS on the Si(111)-(4×1)In reconstruction was similar to our previous work[5] with the exception that 2-keV Li^+ ions were used in the present experiment instead of He^+ ions.

III. RESULTS

A. STM

Figure 1 shows an empty-state image of 1000 Å×1000 Å scan area of the 7×7 reconstruction on a vicinal Si(111) surface with a 2.6° misorientation towards $[\bar{1}\,\bar{1}2]$, i.e., the type-*A* surface. The step edges are along the $[\bar{1}10]$ direction. All the steps except two have single-atom height, i.e., 3.1 Å in this image and the terrace widths are ~100 Å. The other two steps have triple-atom height. After deposition of In on this surface followed by the annealing procedure, a single domain of the 4×1 reconstruction with the double rows parallel to the step edges appears on the terraces as shown in the filled state image of Fig. 2. We found that if the terrace width on the type-*A* surface exceeded ~300 Å, then all three 4×1 domains began to appear. A high-resolution STM image shown in Fig. 3 reveals the double-row structure of the 4×1 reconstruction similar to that reported by Nogami and co-workers.[3,4] The perpendicular spacing between the rows within a double row is 5.6±0.4 Å while the spacing between a pair of double rows is 13.1±0.7 Å.

In contrast to the single domains on the type-*A* surface, STM images exhibit three 4×1 domains aligned with the equivalent $\langle\bar{1}10\rangle$ directions (Fig. 4) on type-*B* surfaces containing terraces ranging in widths from 100 to 500 Å. The existence of three domains on the type-*B*

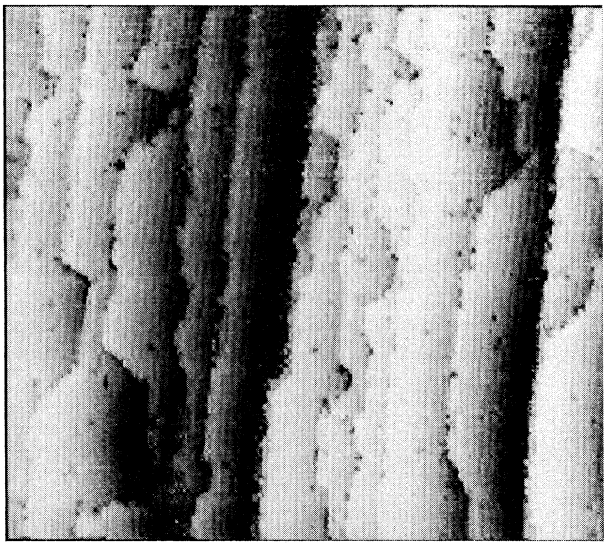

FIG. 2. A 1000 Å×1000 Å filled-state image of the Si(111)-(4×1)In reconstruction showing a single domain of double rows aligned with the $[\bar{1}10]$ step edge direction on the type-*A* vicinal surface as shown in Fig. 1.

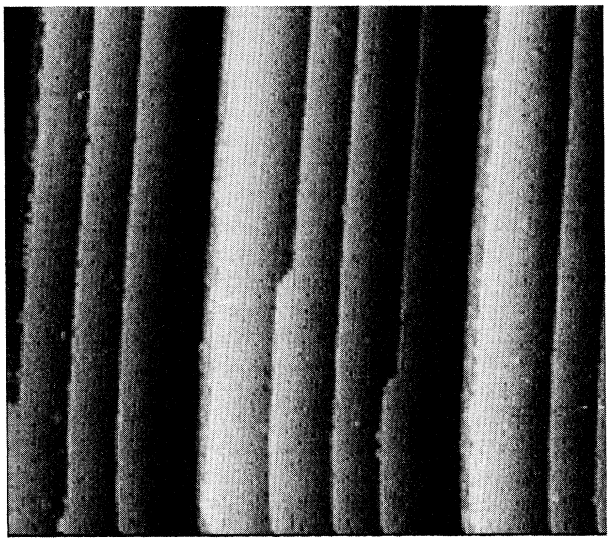

FIG. 1. A 1000 Å×1000 Å empty-state image of the (7×7) reconstruction on a vicinal Si(111) surface. The surface is misoriented by 2.6° towards the $[\bar{1}\,\bar{1}2]$, referred to as the type-*A* surface in the text. The step edges are along the $[\bar{1}10]$ direction.

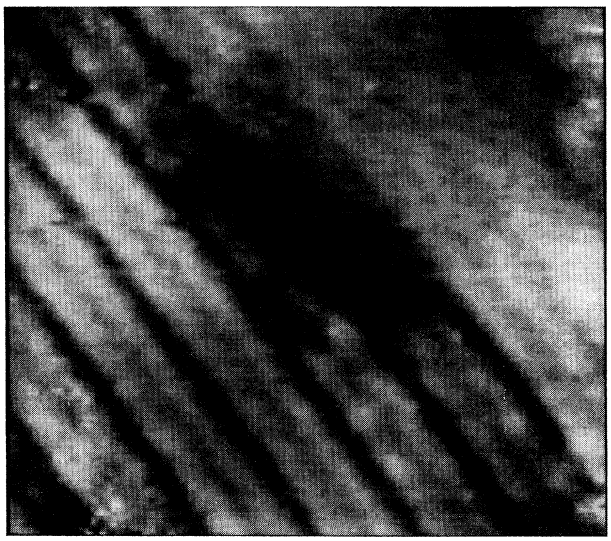

FIG. 3. A 90 Å×90 Å filled-state image of the (4×1) double rows with atomic corrugation.

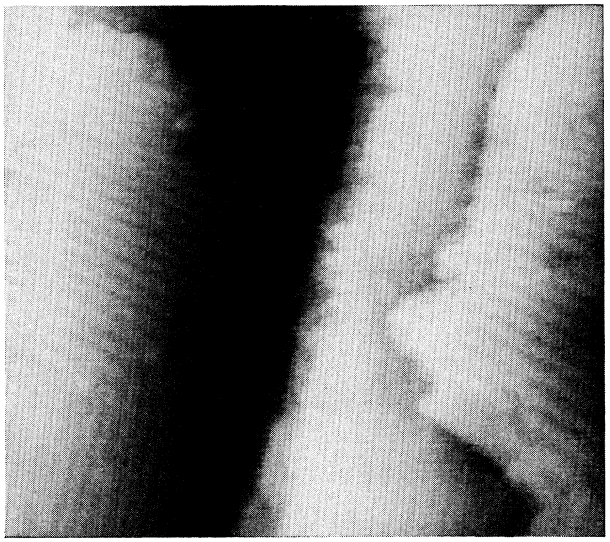

FIG. 4. A 500 Å×500 Å filled-state image of the (4×1) reconstruction showing three domains on a surface misoriented by 2.6° towards the $[11\bar{2}]$ direction, i.e., the type-*B* vicinal surface. The three (4×1) domains are aligned with the equivalent $\langle\bar{1}10\rangle$ directions.

vicinal surface is similar to that observed on a flat surface.[3,4]

Scanning tunneling spectroscopy was also conducted on the 4×1 surface. Figure 5 shows a $(dI/dV)/(I/V)$ versus energy curve obtained by averaging over 100 Å×100 Å area where current imaging tunneling spectroscopy (CITS) (Ref. 12) was performed. This curve corresponds closely to the surface density of states[13] and it shows a band gap of ~0.8 eV, indicating that the 4×1 surface is semiconducting.

B. ICISS

Polar-angle scans for 2-keV Li^+ ions backscattered (scattering angle 163°) from the In adatoms were taken for azimuths along $[\bar{1}10]$, $[\bar{2}11]$, $[\bar{1}01]$, and $[\bar{1}\,\bar{1}2]$ for the type-*A* vicinal surface. Prior to every scan, a LEED pattern of the surface was taken to confirm the existence of only a single 4×1 domain. The polar scans for the four azimuths are shown in Figs. 6, 7, 8, and 9 respectively.

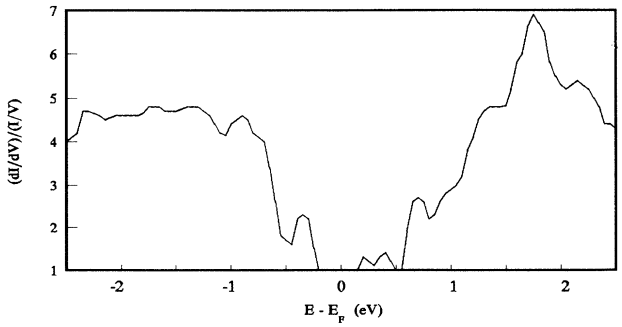

FIG. 5. A tunneling spectrum $(dI/dV)/(I/V)$ as a function of energy, of the Si(111)-(4×1)In reconstruction. This spectrum is obtained by averaging 128×128 *I-V* curves over a 100 Å×100 Å scan during CITS operation.

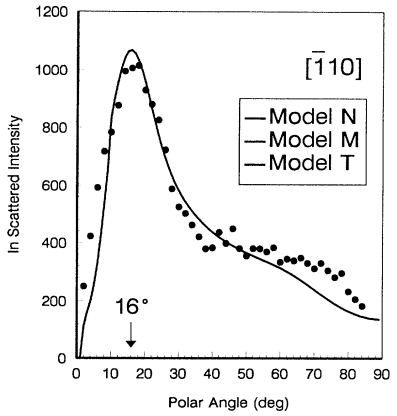

FIG. 6. ICISS polar-angle scan for 2-keV Li^+ ions backscattering from In atoms along the $[\bar{1}10]$ azimuth. The simulations for all three structural models are identical along this azimuth and are shown in a single solid curve.

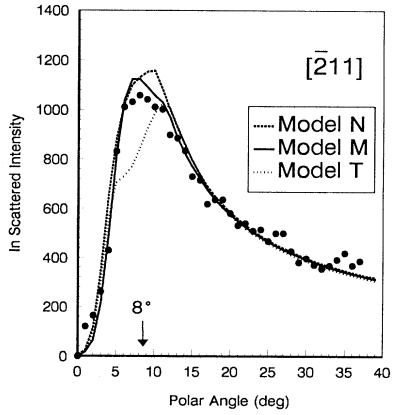

FIG. 7. ICISS polar-angle scan for 2-kev Li^+ ions backscattered from In atoms along the $[\bar{2}11]$ azimuth. The simulations for the three models are shown as three separate curves.

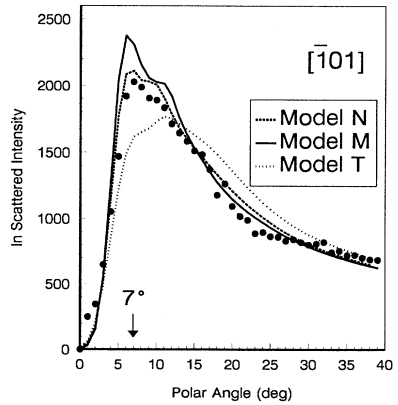

FIG. 8. ICISS polar-angle scan for 2-keV Li^+ ions backscattered from In atoms along the $[\bar{1}01]$ azimuth. The simulations for the three models are shown as three separate curves.

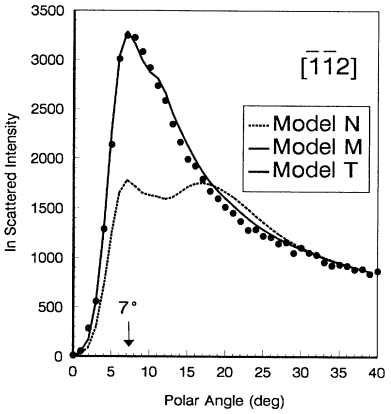

FIG. 9. ICISS polar-angle scan for 2-ke Li^+ ions backscattered from In atoms along the $[\bar{1}\,\bar{1}2]$ azimuth. The simulation for model N is shown as a dotted curve, while the simulation for models M and T are identical and are shown as a solid curve.

All scans were performed in 1° increments from 0° to 90° polar angle (measured between the surface and the incident direction of the ion beam). Figure 6 shows a full 0° to 90° scan along the $[\bar{1}10]$ azimuth with the data points plotted at 2° increments for clarity. This scan, and also scans along other azimuths, show no high-angle shadowing conditions. Therefore we show scans up to 40° only, but with data points at 1° intervals for the other three azimuths in Figs. 7, 8, and 9.

We used 2-keV Li^+ ions instead of He^+ ions because computer simulations for ICISS are easier with Li^+ ions since neutralization factors need not be included. Scattering with Li^+ ions is especially convenient for complex reconstructions at higher coverages, such as the present 4×1 case and the Si(111)-$(2\sqrt{3}\times 2\sqrt{3})$Sn which we have studied recently.[14] Other research groups, notably that of Williams at UCLA,[15] have used Li^+ ion scattering successfully for some time.

IV. DISCUSSION

Both STM images and LEED patterns clearly show the existence of a single (4×1)In domain on the type-A vicinal surface, i.e., with misorientation towards the $[\bar{1}\,\bar{1}2]$ direction. Interpretation of the ICISS polar-angle scans is greatly simplified with the single domain. The scans shown in Figs. 6–9 are fitted to those structural models which are considered to be most likely. They are as follows: (a) The model proposed by Nakamura, Anno, and Kono[8] which will be called model N here, consisting of quadruple atom rows as shown in Fig. 10. The In adatoms reside in H_3 sites on one outside row and in T_4 sites on the other outside row. The In atoms in the two interior rows, which are located 0.8±0.2 Å lower than the outside rows, reside at slightly off bridge sites. The coverage for model N is 1 ML and there are four In adatoms per unit cell, as shown in Fig. 10. (b) The mixed-site model, model M, proposed by us based on our earlier ICISS work on the three-domain 4×1 structure.[5] This model consists of nonequivalent double atom rows with one row of In adatoms residing on H_3 sites while the other row of

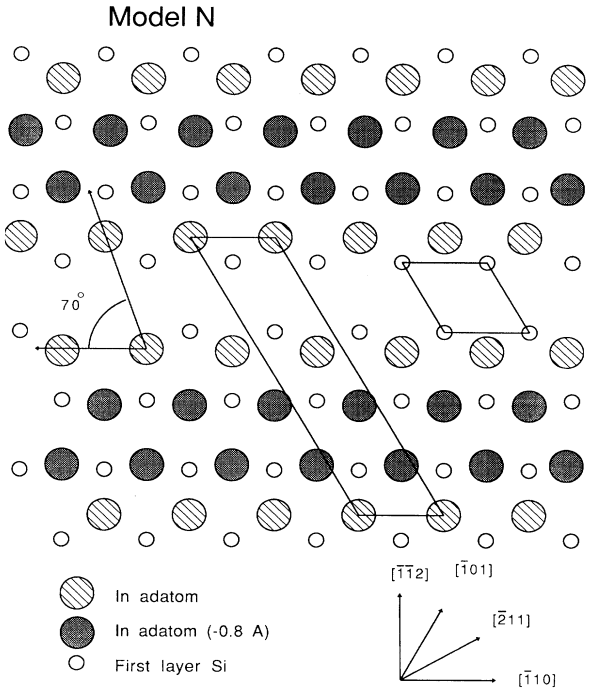

FIG. 10. Schematic plan view of model N, attributed to Nakamura, Anno, and Kono (Ref. 8), of the Si(111)-(4×1)In surface. The first-layer In atoms sit in both H_3 and T_4 sites. The second-layer In atoms sit in bridge sites, 0.8±0.2 Å below the first layer. The coverage is 1 ML. The 1×1 and 4×1 unit cells are outlined.

atoms resides on T_4 sites. The coverage is 0.5 ML and there are two In atoms per unit cell as shown in Fig. 11. (c) The equivalent site model, consisting of double atom rows, with all In adatoms residing in T_4 sites as shown in Fig. 12. This model will be called model T, which also has 0.5 ML coverage.

There are other models for the 4×1 structure. Several of them have been tested previously[5] and found to be unfavorable. In the present work, only the three models N, M, and T are tested for best fits to the ICISS polar-angle scans in Figs. 6–9.

Figure 6 shows a polar-angle scan along the $[\bar{1}10]$ azimuth. From the models N, M, and T shown in Figs. 10, 11, and 12, respectively, it is clear that the only shadowing condition for backscattering from In atoms along the $[\bar{1}10]$ azimuth is the In-In shadowing distance of 3.84 Å. Thus, computer simulations of the polar-angle scans for all three models produce a single solid curve as shown in Fig. 6, which agrees well with the experimental data points. All the curves shown in Figs. 6–9 are generated by a computer simulation procedure in which the backscattered ion intensity is represented by the hitting probability in a two-atom model proposed by Tromp and van der Veen.[16] The simulation incorporates the thermal vibrations of the atoms (0.26 Å for In). A scaling factor of 0.7 is used for Li^+ ions in calculating the Fermi screening radius in the Moliere potential.[17]

The polar-angle scan along the $[\bar{2}11]$ azimuth (Fig. 7) shows a broad peak centered around 8°. The simulation

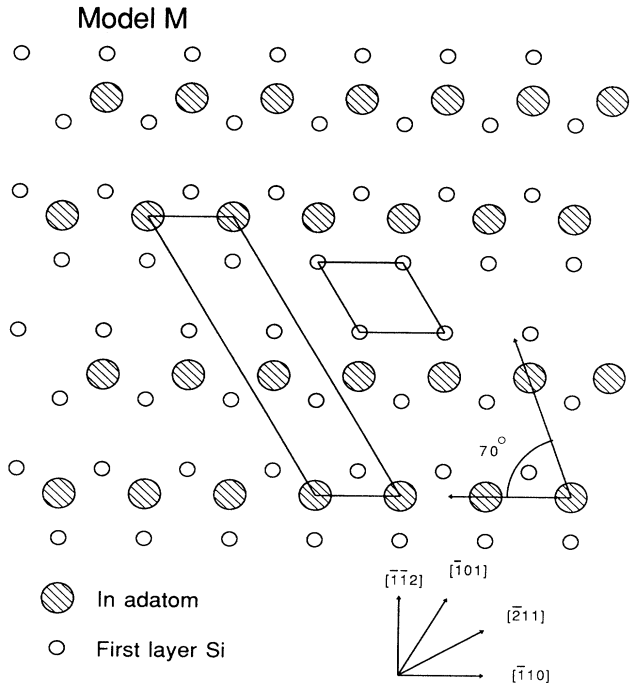

FIG. 11. Schematic plan view of model M, the mixed site model (Ref. 5), of the Si(111)-(4×1)In surface. The In adatoms occupy both H_3 and T_4 sites. The coverage is 0.5 ML. The 1×1 and 4×1 unit cells are outlined.

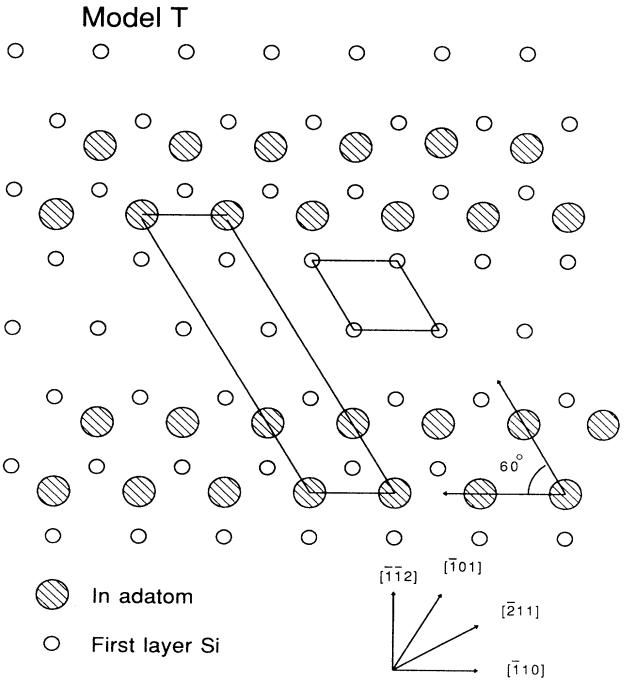

FIG. 12. Schematic plan view of model T, where the In adatoms occupy T_4 sites only. The coverage is 0.5 ML. The 1×1 and 4×1 unit cells are outlined.

of backscattered Li^+ ion intensity from surface In atoms in model N (Fig. 10) consists of four separate shadowing conditions. The In atoms in the H_3 and T_4 sites on the top layer give shadowing distances of 11.1 and 15.5 Å. The In atoms in the bridge sites in the slightly lower (0.8±0.2 Å) layer yield shadowing distances of 6.65 and 20.0 Å. These four shadowing conditions merge together to produce a simulated curve in Fig. 7 with one peak at 10°. Model N shows reasonable agreement with experiment along the [$\bar{2}$11] azimuth. Model M (Fig. 11) only has two shadowing conditions along this azimuth, at 11.1 and 15.5 Å. These two conditions combine to give one peak at 8° in the simulated curve shown in Fig. 7. Model M thus agrees well with experiment. Model T in Fig. 12 gives two shadowing conditions at distances 6.65 and 20.0 Å along the [$\bar{2}$11] azimuth. The simulation for this model shown in Fig. 7 does not provide good agreement with experiment.

A prominent shadowing peak at 7° is apparent in Fig. 8 for the polar-angle scan along the [$\bar{1}$01] azimuth. Model N is Fig. 10 shows one shadowing condition for the top-layer In adatoms separated by a distance of 15.36 Å, and three shadowing distances for the lower bridge-site In atoms at 3.84, 11.52, and 15.36 Å. The three longer shadowing distances, one at 11.52 Å and two at 15.36 Å, produce a merged peak and shoulder between 5° and 10° for the simulation of model N, as shown in Fig. 8. The 3.84-Å condition produces a slight enhancement in backscattered intensity at approximately 18°. It is, however, not very obvious since it represents only one-fourth of the simulation and is overwhelmed by the tails of the other scattering conditions present. Nonetheless, model N shows good agreement with experiment. Model M in Fig. 11 shows two shadowing distances of 15.36 Å along the [$\bar{1}$01] azimuth for the In adatoms. This produces a peak around 7° for the simulated curve which agrees well with experiment, although the peak-to-tail ratio of the curve is larger than that of the experiment. Model T in Fig. 12, with shadowing conditions at 3.84, 11.52, and 15.36 Å, produces a simulated polar-angle scan curve which does not agree well with experiment as shown in Fig. 8.

The largest difference in shadowing conditions shows up along the [$\bar{1}\bar{1}$2] azimuth. Model N in Fig. 10 produces four shadowing distances: two at 13.3 Å with no height difference; one at 5.55 Å and another at 7.77 Å with a height difference of 0.8 Å. The simulated polar-angle scan curve of model N is shown in Fig. 9, displaying a peak at 18° due to the blending together of the shadowing conditions with the height difference. Model N does not agree well with the experimental scan. On the other hand, both model M and model T, consisting only of a single shadowing condition at 13.3 Å, produce a simulated curve which shows excellent agreement with experiment as shown in Fig. 9.

Based on the above comparison of ICISS results and computer simulations, we conclude that model M provides the best description of the Si(111)-(4×1)In reconstruction. The spectroscopy data shown in Fig. 5 also favor model M slightly over model N. Both models have an even number of electrons per unit cell, suggesting that both are semiconducting, in agreement with the

$(dI/dV)/(I/V)$ curve in Fig. 5, showing a band gap of ~ 0.8 eV. However, the $\frac{1}{2}$-ML model M is slightly favored inasmuch as the In adatoms saturate, one for one, all Si dangling bonds. Electronic structure calculations based on these two models can provide a definitive answer.

The remaining question in the present work is why is there a difference between the 4×1 reconstructions on the type-A, i.e., surface normal tilted towards $[\bar{1}\,\bar{1}2]$) and type-B (i.e., towards $[11\bar{2}]$) vicinal surfaces. We observe a single 4×1 domain on the type-A surface, whereas three 4×1 equivalent domains exist on type B. On the type-A surface, all the 4×1 double rows are aligned along the step edges in the $[\bar{1}10]$ direction as shown in the STM image of Fig. 2. We propose a model of the type-A and type-B step edges which may explain the difference in the 4×1 reconstructions. This is represented by a side view and a plan view of a single-domain 4×1 reconstruction in the vicinity of the step edges as shown in Figs. 13 and 14, respectively. Measurements of the corrugation of the STM image in Fig. 3 indicate that the In adatoms are situated 1.5 ± 0.2 Å above the Si(111) surface. The nearest distance between an In adatom and a Si atom on the type-A step edge is 4.42 Å with a height difference of 1.6 Å as shown in Figs. 13(a) and 14. On the type-B vicinal surface where all three equivalent domains coexist, the nearest distance between an In adatom on a (4×1) row parallel to the step edge and a Si atom on the step edge is 5.58 Å with a height difference of 0.8 Å, as shown in Figs. 13(b) and 14. It is conceivable that the closer proximity of the In adatom to the type-A step edge promotes single-domain reconstruction. It should be noted that our proposed model of the step edges is nonunique, but other configurations do not produce the proximity argument presented here. Total-energy calculations of the two situations will clarify the understanding of the preference of type-A vicinal surfaces over type-B vicinal surfaces for the formation of a single 4×1 domain.

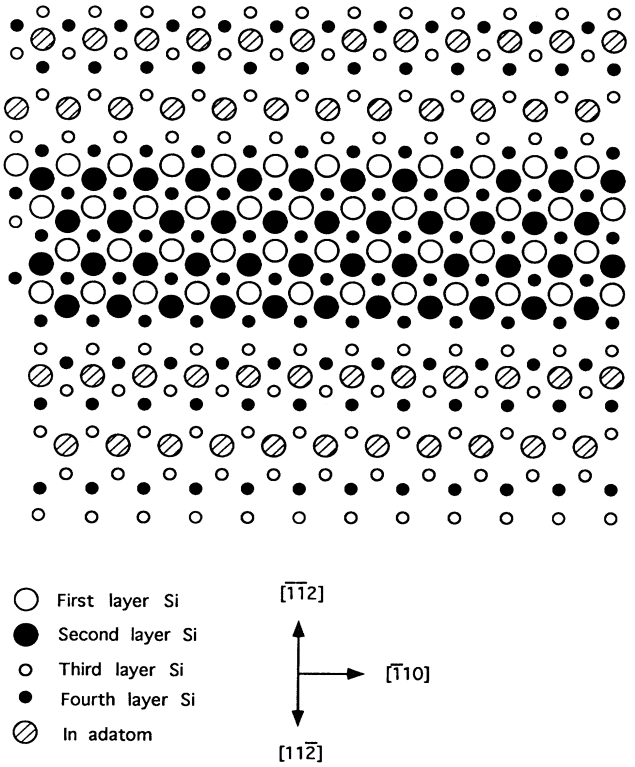

FIG. 14. Schematic plan view of the (4×1)In double rows aligned with the $[\bar{1}10]$ step-edge direction near the type-A and type-B steps. The In double rows are omitted on the upper terrace for clarity.

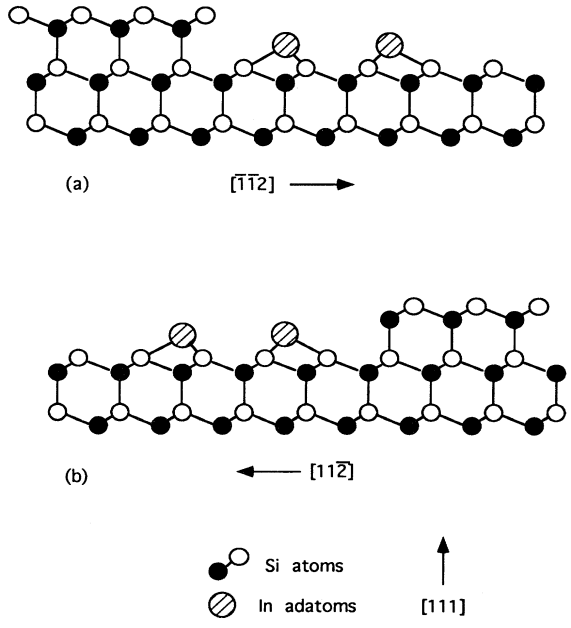

FIG. 13. Schematic side view of the (4×1)In double rows located near the edge of the Si(111) vicinal surface: (a) outward normal of step is the $[\bar{1}\,\bar{1}2]$ direction (type A in text), and (b) outward normal of step is the $[11\bar{2}]$ direction (type B in text).

An alternative explanation for the contrasting behavior observed in the two orientations is due to the difference in surface strains that partially underlie the very different step-step interactions seen on these two oriented surfaces.[18] A more isotropic strain field would favor multiple domain growth.

V. CONCLUSIONS

STM images show that a single domain of the (4×1)In reconstruction is present on Si(111) vicinal surfaces (type A) misoriented at 2.6° towards $[\bar{1}\,\bar{1}2]$. ICISS polar scans taken on such a surface provide the best agreement with computer simulations based on a mixed-site, i.e., H_3 and T_4 sites, model with 0.5-ML coverage, confirming our previous ICISS results on a three domain 4×1 surface.[5] For Si(111) vicinal surfaces misoriented

towards $[11\bar{2}]$, however, a three-domain 4×1 reconstruction similar to that found on flat Si(111) surfaces is present. The preference of a single-domain formation on type-*A* vicinal surfaces is attributed to the proposition that the In adatoms are located nearer to the type-*A* step edge than the type-*B* step edge.

ACKNOWLEDGMENTS

We thank Brian S. Swartzentruber for the supply of samples of Si(111) vicinal surfaces. This work was supported by the National Science Foundation under Grant No. DMR-9116505.

[1]J. J. Lander and J. Morrison, Surf. Sci. **2**, 553 (1964).
[2]J. J. Lander and J. Morrison, J. Appl. Phys. **36**, 1706 (1965).
[3]J. Nogami, S. I. Park, and C. F. Quate, Phys. Rev. B **36**, 6221 (1987).
[4]S. I. Park, J. Nogami, and C. F. Quate, J. Microsc. **152**, 727 (1988).
[5]D. M. Cornelison, M. S. Worthington, and I. S. T. Tsong, Phys. Rev. B **43**, 4051 (1991).
[6]S. Baba, H. Hirayama, J. M. Zhou, and A. Kinbara, Thin Solid Films **90**, 57 (1982).
[7]M. Kawaji, S. Baba, and A. Kinbara, Appl. Phys. Lett. **34**, 748 (1979).
[8]N. Nakamura, K. Anno, and S. Kono, Surf. Sci. **256**, 129 (1991).
[9]E. Bauer (private communication).
[10]G. Akinci, T. R. Ohno, and E. D. Williams, Surf. Sci. **201**, 27 (1988).
[11]E. D. Williams and N. C. Bartelt, Science **251**, 393 (1991).
[12]R. J. Hamers, R. M. Tromp, and J. E. Demuth, Phys. Rev. Lett. **56**, 1972 (1986).
[13]R. M. Feenstra, J. A. Stroscio, and A. P. Fein, Surf. Sci. **181**, 295 (1987).
[14]M. S. Worthington, J. L. Stevens, C. S. Chang, and I. S. T. Tsong, J. Vac. Sci. Technol. A **10**, 657 (1992).
[15]J. H. Huang, and R. S. Williams, Phys. Rev. B **38**, 4022 (1988).
[16]R. M. Tromp and J. F. van der Veen, Surf. Sci. **133**, 159 (1983).
[17]C. S. Chang, U. Knipping, and I. S. T. Tsong, Nucl. Instrum. Methods B **18**, 11 (1986).
[18]X. -S. Wang, J. L. Goldberg, N. C. Bartelt, T. L. Einstein, and Ellen D. Williams, Phys. Rev. Lett. **65**, 2430 (1990).

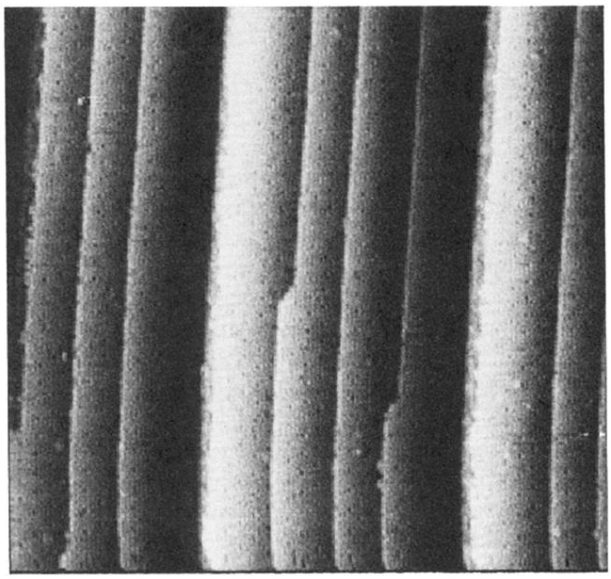

FIG. 1. A 1000 Å × 1000 Å empty-state image of the (7×7) reconstruction on a vicinal Si(111) surface. The surface is misoriented by 2.6° towards the $[\bar{1}\,\bar{1}2]$, referred to as the type-*A* surface in the text. The step edges are along the $[\bar{1}10]$ direction.

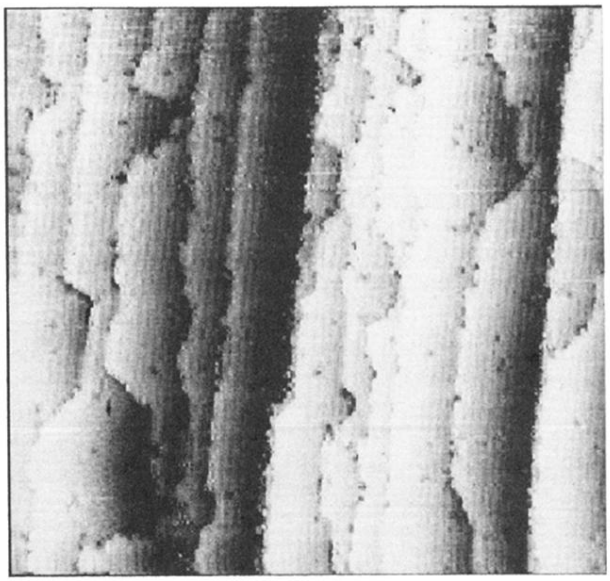

FIG. 2. A 1000 Å × 1000 Å filled-state image of the Si(111)-(4×1)In reconstruction showing a single domain of double rows aligned with the $[\bar{1}10]$ step edge direction on the type-*A* vicinal surface as shown in Fig. 1.

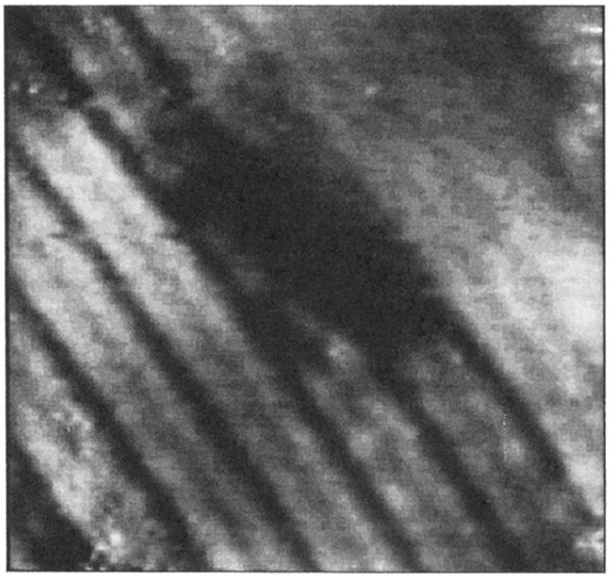

FIG. 3. A 90 Å×90 Å filled-state image of the (4×1) double rows with atomic corrugation.

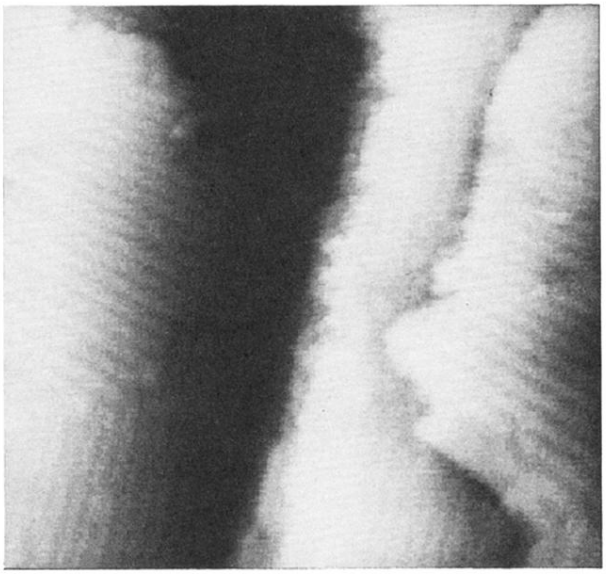

FIG. 4. A 500 Å$\times$500 Å filled-state image of the (4$\times$1) reconstruction showing three domains on a surface misoriented by 2.6° towards the [11$\bar{2}$] direction, i.e., the type-*B* vicinal surface. The three (4$\times$1) domains are aligned with the equivalent $\langle \bar{1}10 \rangle$ directions.